White matter hyperintensity-associated structural disconnection, resting state functional connectivity, and cognitive control in older adults

Abhishek Jaywant[a,b], Katharine Dunlop[a,c], Lindsay W. Victoria[a,d], Lauren Oberlin[a,d], Charles Lynch[a,c], Matteo Respino[a,d], Amy Kuceyeski[e], Matthew Scult[a], Matthew Hoptman[f,g], Conor Liston[a,c], Michael W. O'Dell[b], George S. Alexopoulos[a,d], and Faith M. Gunning[a,d]

[a]Department of Psychiatry, Weill Cornell Medicine, 525 E 68th St, New York, NY 10065, USA.
[b]Department of Rehabilitation Medicine, Weill Cornell Medicine, 525 E 68th St, New York, NY 10065, USA.
[c]Feil Family Brain and Mind Research Institute, Weill Cornell Medicine, 413 East 69th St, New York, NY, 10021, USA.
[d]Weill Cornell Institute of Geriatric Psychiatry, 21 Bloomingdale Road, White Plains, NY 10605, USA.
[e]Department of Radiology, Weill Cornell Medicine, 525 E 68th St, New York, NY 10065, USA.
[f]Nathan Kline Institute, 140 Old Orangeburg Road, Orangeburg, NY 10962, USA.
[g]Department of Psychiatry, NYU School of Medicine, 550 First Avenue, New York, NY, 10016, USA.

Corresponding author:
Faith M. Gunning, Ph.D.
Fgd2002@med.cornell.edu
525 E 68th St, New York, NY, 10065

Declarations of interest: none

Abbreviations: ARWMC = Age-Related White Matter Change scale; ChaCo = Change in Connectivity; DMN = Default Mode Network; FDR = False Discovery Rate; HVLT-R = Hopkins Verbal Learning Test-Revised; PLSR = Partial Least Square Regression; RSFC = Resting State Functional Connectivity; TMT = Trail Making Test; TMT-B/A = Trail Making Test, ratio of B over A; VIP = Variable importance in the projection; WMH = White Matter Hyperintensities.

Abstract

White matter hyperintensities (WMH) are linked to cognitive control; however, the structural and functional mechanisms are largely unknown. We investigated the relationship between WMH-associated disruptions of structural connectivity, resting state functional connectivity (RSFC), and cognitive control in older adults. Fifty-eight cognitively-healthy older adults completed cognitive control tasks, structural MRI, and resting state fMRI scans. We estimated inferred, WMH-related disruptions in structural connectivity between pairs of subcortical and cortical regions by overlaying each participant's WMH mask on a normative tractogram dataset. For region-pairs in which structural disconnection was associated with cognitive control, we calculated RSFC between nodes in those same regions. WMH-related structural disconnection and RSFC in the cognitive control network and default mode network were both associated with poorer cognitive inhibition. These regionally-specific, WMH-related structural and functional changes were more strongly associated with cognitive inhibition compared to standard rating of WMH burden. Our findings highlight the role of circuit-level disruptions to the cognitive control network and default mode network that are related to WMH and impact cognitive control in aging.

MeSH Keywords

Cognitive Aging; Neuropsychology; Neuroimaging; Magnetic Resonance Imaging; Cerebrovascular disease

1. Introduction

Cerebrovascular disease is common in older adults, associated with poor health outcomes (Debette and Markus, 2010), and characterized by neurobiological abnormalities such as white matter hyperintensities (WMH) (Moroni et al., 2018). WMH are associated with cognitive decline in older adults; a potential mechanism is the WMH lesions' impact on structural connectivity (Langen et al., 2018). WMH affect the strength and efficiency of white matter connections, i.e. the structural connectome, which in turn are associated with slower processing speed (Tuladhar et al., 2016) and declines in reasoning, working memory, episodic memory, and cognitive flexibility (Gunning-Dixon and Raz, 2003; Wiseman et al., 2018).

Cognitive control—the ability to maintain task-relevant information in mind, flexibly shift set, and inhibit irrelevant information—is especially susceptible to cerebrovascular disease and WMH and their impact on structural connectivity. In older adults, cognitive control functions are linked to structural disconnection in frontal-subcortical circuits (Klostermann et al., 2012) arising from cerebrovascular disease (Pantsiou et al., 2018). These processes and resulting age-related changes in cognitive control have important ramifications for older adults because better cognitive control is tied to greater independence in everyday activities of daily living (Cahn-Weiner et al., 2002; Vaughan and Giovanello, 2010).

Decreased efficiency of cognitive control functions in the setting of cerebrovascular disease may also depend on functional connectivity. Both structural and functional connectivity contribute independently to healthy cognitive aging (Liem et al., 2017). In older adults with small vessel ischemic disease, worse cognitive control is associated with diminished resting state functional connectivity (RSFC) in the frontoparietal network, default mode network (DMN), and in subcortical structures (Schaefer et al., 2014; Sun et al., 2011; Yi et al., 2015). Despite advances in neuroimaging techniques, the interrelationships among neuroimaging markers of cerebrovascular disease (WMH), structural connectivity, and RSFC, and how these interactions may contribute to age-related changes in cognitive control, is largely unknown. The relationship between these processes are important in understanding the mechanisms that underly age-related cognitive decline.

The primary objective of the present study was to investigate how WMH-associated disruptions to structural connectivity and RSFC are related to cognitive control functions in healthy older adults. We used a novel technique via the Network Modification Tool (Kuceyeski et al., 2013) to estimate inferred WMH-associated structural connectivity disruption and its impact on cognitive control. The Network Modification Tool expands on prior studies that have restricted analyses to specific networks (Reijmer et al., 2015; Sun et al., 2011) and that have used coarser methods to quantify WMH burden. We hypothesized that WMH would be associated with structural disconnection within nodes of the cognitive control network and between the cognitive control network and the DMN (Leech and Sharp, 2014; Vatansever et al., 2017). We further hypothesized that greater structural connectivity disruption would be associated with low RSFC, but that structural and functional connectivity measures would each account for unique variance in explaining cognitive control performance. Finally, we explored whether a model that accounted for structural and functional disconnection would more strongly predict cognitive control than a model that used traditional clinical ratings of WMH burden.

2. Materials and Methods

2.1. Participants. Participants were 58 cognitively-healthy, independent, and community-dwelling older adults aged 60-84 (M=72.9 years, SD=6.02) who were enrolled in a larger trial investigating cognitive control and emotion regulation in late-life depression. All participants were English-speaking, non-depressed, and cognitively unimpaired (Mini Mental Status Examination ≥ 26/30) (Folstein et al., 1983). Participants had no current or past history of major psychiatric illness or neurologic disorder. All subjects were recruited through flyers and advertisements. All provided written informed consent, and the study was approved by the Institutional Review Boards of Weill Cornell Medicine and the Nathan Kline Institute. The participants constituted the control group for an analysis on structural connectivity and performance on the Trail Making Test in late-life depression that has been previously published by our group (Respino et al., 2019). We extend our previous work by performing analyses of RSFC and relating region-pair based structural connectome disruption to cognitive control measures.

2.2. Neuropsychological Assessment. Research assistants trained and certified by the Weill Cornell Institute of Geriatric Psychiatry administered the neuropsychological measures. To assess auditory attention and working memory, we administered the Digit Span subtest of the Wechsler Adult Intelligence Scale-Fourth edition (Wechsler, 2008). The total score across the forwards, backwards, and sequencing conditions was used in the analysis. Higher scores indicate greater attention/working memory capacity. The Stroop Color Word Test was used to assess cognitive inhibition and susceptibility to interference from conflicting information (Golden and Freshwater, 2002). The interference index was calculated based on the established formula, *ColorWord – [(Word x Color) / (Word + Color)]*. Lower scores indicate greater difficulty with cognitive inhibition. To assess attentional set-shifting we used the Trail Making Test (TMT) (Reitan, 1958) and calculated a ratio that isolates the shifting component while accounting for psychomotor processing speed, by dividing the time to completion on TMT-B by the time to completion on TMT-A (Salthouse, 2011). Higher scores represent poorer attentional set-shifting. We administered the Hopkins Verbal Learning Test-Revised (Brandt and Benedict, 2001) and used the number of words recalled on the delayed recall trial as a control condition to evaluate the specificity of our findings to cognitive control relative to long-term memory retrieval.

2.3. Neuroimaging. Structural and functional MRI scans were acquired on a 3T Siemens TiM Trio (Erlangen, Germany) scanner that was equipped with a 32-channel head coil at the Center for Biomedical Imaging and Neuromodulation of the Nathan Kline Institute for Psychiatric Research. Structural imaging included high-resolution whole brain images acquired using a 3D T1-weighted MPRAGE and T2-weighted FLAIR images. The acquisition parameters for MPRAGE were: TR = 2500ms, TE = 3.5ms, slice thickness = 1mm, TI = 1200ms, 192 axial slices, matrix = 256 x 256 (voxel size = 1mm isotropic), FOV = 256mm, IPAT = 2, flip angle = 8 degrees. The acquisition parameters for the FLAIR sequence were TR = 9000ms, TE = 111ms, TI = 2500ms, FOV = 192 x 256 mm, matrix 192 x 256, slice thickness = 2.5 mm, number of slices = 64, IPAT = 2, flip angle = 120 degrees. The final FLAIR resolution (rectangular FOV/matrix) was 1x1 in plane. Functional neuroimaging was a turbo dual echoplanar image (EPI) sequence performed while participants were at rest. Acquisition parameters were repetition time = 2500ms, echo time = 30ms, flip angle = 80 degrees, slice thickness = 3mm, 38 axial slices, matrix = 72 x 72, 3-mm isotropic, field of view = 216mm, integrated parallel acquisition

techniques factor = 2. Resting-state image acquisition was conducted in a single run that was 6 minutes and 15 seconds in duration, TR = 2000ms. Participants were instructed to stay awake with eyes closed. Wakefulness was verified at the end of the scanning sequence by the technician.

[Insert Figure 1 about here]

Procedures to segment and estimate WMH burden and to estimate the impact of WMH on structural connectivity disruption have been previously described in detail (Respino et al., 2019). Figure 1 illustrates the flow of neuroimaging analysis and statistical procedures. In brief, two raters performed a visual rating using operational criteria of the Age-Related White Matter Change scale (ARWMC) (Wahlund et al., 2001; Xiong et al., 2011). Inter-rater reliability was strong (Intraclass Correlation Coefficient = .95). FSL (Jenkinson et al., 2012) and the BIANCA program (Griffanti et al., 2016) were subsequently used to segment WMH lesions and create WMH masks. WMH lesions smaller than 3 voxels were removed. A visual check was performed on each individual WMH mask and minimal manual adjustments were made. Each final WMH mask was nonlinearly registered to MNI space and binarized.

WMH-associated, inferred structural dysconnectivity was then estimated using the Network Modification Tool, which has previously been used in aging populations (Kuceyeski et al., 2015, 2013, 2012). Each WMH mask was entered into the program in Matlab R2017b (MathWorks, Natick, MA) and overlaid on a normative sample of 73 healthy subjects' tractograms. The program estimates dysconnectivity by removing those streamlines passing through a subject's WMH mask and recalculating the strength of connections between pairs of regions ("modified connectome"). This procedure is conducted using an 86-region Freesurfer parcellation that includes 68 cortical regions, 16 subcortical regions, and two cerebellar regions. For our analysis, we were interested in the proportional loss in connectivity between pairs of regions. The "dysconnectivity score" was calculated for each region pair by dividing the number of streamlines in that subject's modified connectome by the mean number of streamlines in that region pair from the 73 healthy control tractogram set and subtracting one. Values range from 0 to -1, with more negative values indicating greater disconnection. Because many region pairs

have minimal streamlines so that "loss" of just one or two streamlines could result in a dysconnectivity score of 50-100%, we retained only those region pairs that had at minimum 10 streamlines passing between them, a threshold that has been used in tractography/diffusion tensor imaging in cerebrovascular disease (Xu et al., 2019). This resulted in approximately 20% of the region pairs being retained. To further reduce the dimensionality of the correlation matrix and to reduce noise from regions with minimal dysconnectivity while focusing on those region pairs which the greatest disconnection, we entered into subsequent analyses region pairs that had a dysconnectivity score of at least -.10 (i.e., minimum 10% loss of connectivity). This resulted in 170 region pairs that were retained for our analyses. Note that the use of the terms "dysconnectivity score" and "structural dysconnectivity" in the Results and Discussion refer to inferred dysconnectivity using the above procedure.

To extract corresponding RSFC values for the 170 region pairs with a dysconnectivity score less than or equal to -0.10, each subject's EPI images were motion corrected using FSL's MCFLIRT, linearly registered to the anatomical T1 scan, and normalized to the MNI 152 template. Additional preprocessing including slice-timing correction and spatial smoothing (6mm FWHM) was performed in AFNI (Cox, 1996). Further removal of motion artifacts was performed using ICA-AROMA (Pruim et al., 2015). Motion was regressed out (demeaned and first derivative), artifacts were further removed using AFNI's *anaticor*, and the time-series was bandpass filtered. Time-series data were extracted using a previously published parcellation of 277 functional nodes (Drysdale et al., 2017) that includes the 264 nodes from the Power atlas (Power et al., 2011) combined with 13 additional nodes in the caudate, amygdala, hippocampus, nucleus accumbens, subgenual anterior cingulate, locus coeruleus, ventral tegmental area, and the raphe nucleus. Each subject's 277x277 matrix was Fisher r-to-Z transformed. Note that we elected not to use the same 86-region FreeSurfer parcellation for RSFC because current recommendations suggest using functionally-based parcellations with much more fine-grained nodes for fMRI data (Arslan et al., 2018; Hallquist and Hillary, 2018).

2.4. Statistical Analysis. Statistical analyses were conducted using IBM SPSS Statistics version 25 (IBM, Armonk, NY) and Matlab. Analyses focused on the 170 region pairs calculated as described above. Dysconnectivity scores were normalized to Z-scores for each region pair. These

scores were separately correlated with performance on the neuropsychological measures of cognitive control (Digit Span, Stroop Interference, TMT B/A Ratio) and of memory (HVLT-R Delayed Recall) using Spearman rank-order correlations. Each correlation analysis was FDR-corrected using the Benjamini-Hochberg method with $q < 0.05$; corrected p-values are reported for those correlations that survived significance. For those 170 region pairs that were significantly associated with cognitive measures, we extracted overlapping functional nodes from the modified Power parcellation by calculating the Dice similarity coefficient between functional nodes (Power parcellation 10mm diameter spheres) and structural region pairs (Freesurfer 86-region parcellation). Functional nodes that had a Dice coefficient > 0 (i.e. had > 1 voxel overlapping the structural ROI) were retained. The correlation between their functional connectivity and cognitive measures were calculated. Given that RSFC-cognition correlations were already constrained by selecting only those few nodes that overlapped with the significant structural dysconnectivity scores, we elected not to FDR-correct RSFC-cognition correlations.

To explore the combined effect of structural dysconnectivity and RSFC on cognitive control, relative to a clinical rating of WMH, we computed two partial least square regression (PLSR) models. In the first model, we entered the region pairs in which structural dysconnectivity scores survived FDR correction and were associated with cognitive measures, as well as the overlapping RSFC nodes in those same region pairs that were also significantly associated with cognitive measures. We computed a second PLSR model in which pairwise structural dysconnectivity and RSFC were replaced with the visual rating of WMH burden (ARWMC score). Age and gender were covariates in both models. To minimize model over-fitting, we chose the factor solution that minimized the mean square error using leave-one-out cross-validation. Predictor variables that loaded onto the components of interest were determined by inspecting the variable importance in the projection. Regions of interest that had variable importance values close to or exceeding "1" were considered to contribute to a given component (Mehmood et al., 2012).

[Insert Table 1 and 2 about here]

3. Results

3.1. Demographic and clinical variables. Table 1 displays the mean, SD, and ranges for age, education, and performance on the neuropsychological measures for our sample. The ratio of male:female participants is also provided.

3.2. Correlations between WMH-linked dysconnectivity score and behavior. Figure 2 demonstrates the relationship between all 170 region pairs and Stroop Interference, while Table 2 and Figures 3 and 4 illustrate how the dysconnectivity score in sixteen region pairs demonstrated significant correlations with Stroop Interference. These region pairs primarily encompassed subcortical (caudate, thalamus, pallidum)-cortical disconnections, which were associated with poorer cognitive inhibition on the Stroop task. Regions included connections between subcortical nodes and regions of the cognitive control network, DMN, and sensorimotor network. No correlations survived FDR-correction for Digit Span, TMT B/A Ratio, or HVLT-R Delayed Recall.

[Insert Figure 2, 3, and 4 about here]

3.3. Correlations between RSFC and cognitive performance. As shown in Table 2 and Figure 5, RSFC in functional nodes within these sixteen region pairs demonstrated significant correlations with Stroop Interference. Specifically, cognitive inhibition was positively correlated with RSFC between the right caudate and nodes in the right superior parietal, right inferior parietal, right caudal middle frontal, and right precentral regions. Cognitive inhibition was negatively correlated with RSFC between the left inferior frontal gyrus/pars triangularis and left medial orbitofrontal cortex, between the right caudate and a node overlapping the right posterior cingulate/supramarginal/postcentral region, and between the right pallidum and right superior frontal region.

3.4. Correlations between Structural Dysconnectivity Score and RSFC. Table 2 also shows the correlations between structural dysconnectivity and RSFC for the sixteen region pairs in which dysconnectivity score was associated with Stroop Interference. Greater structural dysconnectivity was associated with lower RSFC between the right caudate and right precentral gyrus. The

remaining correlations between structural dysconnectivity score and RSFC in the 16 region pairs were not significant.

[Insert Figure 5 about here]

3.5. Exploratory PLSR models. For the first model that incorporated the structural and functional region-pairs that were associated with Stroop Interference above, results indicated a one-factor solution that accounted for 14% of the variance in Stroop Interference performance. The factor was comprised primarily of WMH-related dysconnectivity in subcortical-cortical and cortical-cortical region pairs of the cognitive control network, DMN, and sensorimotor network. The factor also comprised RSFC between the right caudate and a functional node spanning the right supramarginal/posterior cingulate/postcentral region, and between the right caudate and right inferior parietal region. An analogous PLSR model that replaced pairwise structural and functional connectivity with the ARWMC score (visual rating of WMH), accounted for only 5% of variance in Stroop Interference performance.

4. Discussion

The principal finding of this study is that WMH-related inferred structural dysconnectivity and resting state functional connectivity are associated with cognitive inhibition and the ability to resolve interference from competing information in older adults. The strength of both structural and functional connections that link subcortical regions to nodes of the cognitive control network and default mode network are associated with cognitive inhibition. Our findings indicate that aging-related alterations in structural and functional circuitry are both associated with declines in select aspects of cognitive functioning.

Our examination of WMH-related structural dysconnectivity replicates prior studies demonstrating a relationship between disruptions in white matter pathways and age-related cognitive decline (Tuladhar et al., 2016; Wiseman et al., 2018), and extends them to identify specific regions in the cognitive control network. The implicated regions are those important to attentional control (superior and inferior parietal cortex), and conflict monitoring and error detection (anterior cingulate cortex) (Braver et al., 2001; Gasquoine, 2013), processes that are

assessed by the Stroop task. Dysconnectivity between these cognitive control regions and regions of the caudate and thalamus are consistent with the premise that frontal-striatal-thalamocortical connections are necessary to support efficient cognitive control (de la Fuente-Fernández, 2012).

WMH-associated structural disconnection in nodes of the DMN (posterior cingulate, left medial frontal cortex) and poorer cognitive inhibition were also observed in our analyses. This finding is consistent with the known role of the DMN in cognitive control processes, supported by dense connections of DMN structures with nodes of the cognitive control network, including the dorsolateral prefrontal cortex (Leech and Sharp, 2014). The DMN may support cognitive control performance via goal formation and task preparation in anticipation of engaging in cognitively demanding tasks (Koshino et al., 2014).

We also examined resting state functional connectivity between the regions with disruptions in structural connectivity in the cognitive control network and DMN. Although we did not observe significant correlations between structural dysconnectivity and RSFC in these region-pairs, we did find a link between RSFC and cognitive performance. Higher RSFC within several nodes of the cognitive control network was associated with greater cognitive inhibition. Specifically, we observed positive correlations between Stroop task performance and RSFC between the caudate and nodes in the superior parietal, inferior parietal, and caudal middle frontal regions. These regions are encompassed within the frontoparietal task control network as originally delineated by Power et al. (2011). Thus, our findings suggest that WMH-related structural dysconnectivity and lower RSFC between the caudate and nodes of the frontoparietal network are both associated with poorer cognitive inhibition and contribute to a diminished ability to ignore distracting information and attend to task-relevant information in healthy older adults.

In contrast to the positive correlations between resting state functional connectivity of frontoparietal region-pairs in the cognitive control network and cognitive inhibition, we observed negative correlations between cognitive inhibition and RSFC in nodes of the DMN. That is, better cognitive inhibition was associated with *lower* functional connectivity between (1) the caudate and posterior cingulate/supramarginal/postcentral region (sensorimotor/DMN), (2) the pallidum and a node in the superior frontal region within the DMN (Power et al., 2011), and (3)

the inferior frontal gyrus pars triangularis (frontoparietal node) and medial orbitofrontal cortex (DMN). This finding is consistent with the function of the DMN as a “task negative” network and that greater anti-correlation between the cognitive control network (which subsumes the frontoparietal task control network) and DMN is beneficial for cognitive performance (Chen et al., 2013) and healthy cognitive aging (Esposito et al., 2018).

The relationship between WMH, structural connectivity, and resting state functional connectivity and their mechanistic contribution to age-related cognitive decline is largely unknown. Here, we demonstrate that inferred structural dysconnectivity and alterations in resting state functional connectivity in the cognitive control network and DMN are both associated with poorer cognitive inhibition in healthy aging. These findings highlight the role of disruptions in circuit-level connections that are driven by WMH in cognitive aging. That structural dysconnectivity and functional connectivity were both related to cognitive inhibition, and largely did not correlate with one another, is consistent with the known decrease in structure-function coupling in older adults (Zimmermann et al., 2016), in psychiatric disease (Skudlarski et al., 2010), and in the presence of WMH burden (Reijmer et al., 2015). Our results also align with prior work demonstrating the independent involvement of task-evoked functional activity and white matter integrity in normal appearing white matter in age-related memory and executive function decline (de Chastelaine et al., 2011). Our findings suggest that in regions with inferred structural disconnection due to WMH, functional connections between those regions remain relevant to cognitive inhibition.

WMH-related structural and functional connectivity also accounted for greater variance in cognitive inhibition performance than did a traditional clinical measure (visual rating) of WMH burden. By estimating regionally-specific network changes associated with WMH, the Network Modification Tool may detect subtle variations in cognitive performance not captured by conventional global indicators of WMH burden. Moreover, by leveraging a normative tractogram reference dataset, the Network Modification Tool does not require diffusion weighted imaging, and may be a more scalable and cost effective approach to estimating the network impact of WMH.

Although WMH-related structural dysconnectivity and resting state functional connectivity predicted cognitive inhibition on the Stroop task, we did not find significant associations with other aspects of cognitive control such as set-shifting (TMT B/A) and auditory attention and working memory (Digit Span), nor on a measure of verbal memory recall (Hopkins Verbal Learning Test). Cognitive control is not a unitary construct and is comprised of specific processes including updating, inhibition, and set-shifting (Friedman and Miyake, 2017), suggesting that our findings apply more to the conflict monitoring and inhibition aspect of cognitive control than to shifting or updating/working memory. The lack of association with working memory may be related to the assessment itself, as the Digit Span may not be as sensitive to working memory as tasks that place greater demands on rapid updating and manipulation of information under time constraints (Tombaugh, 2006).

The limitations of the present study include the length of the resting state scan (6 minutes and 15 seconds), which was of short duration compared to current standards. Given that reliability tends to increase with longer durations (Zuo and Xing, 2014) replication of our RSFC findings with longer scan times is warranted. Further, our age range was relatively restricted and future studies would benefit from including a broader range of ages and comparing our findings to middle-aged and old-old adults.

4.1. Conclusion

We demonstrate that in cognitively healthy older adults, cerebrovascular disease (WMH)-related inferred structural dysconnectivity and resting state functional connectivity in cortical and subcortical regions of the cognitive control and default mode networks are both associated with cognitive inhibition and conflict monitoring. Our findings highlight the role that alterations in the structural and functional connectome both play in cognitive aging in the setting of cerebrovascular disease.

Acknowledgements

We thank Cristina Pollari for assistance with database management and Naib Chowdhury for help acquiring behavioral data. We also thank Elvisha Dhamala for assistance in creating the figures. This work was supported by the National Institute of Mental Health (NIMH) grants R01 MH097735 (Gunning) and T32 MH019132 (Alexopoulos). The sponsor did not have any role in the study design, the acquisition, analysis, or interpretation of the data, the writing of the report, or the decision to submit the manuscript for publication.

Financial Disclosures/Conflicts of Interest

G.S. Alexopoulos has served on the speakers' bureaus of Allergan, Otsuka, and Takeda-Lundbeck and on advisory groups for Janssen and Eisai. Drs. Jaywant, Dunlop, Victoria, Oberlin, Lynch, Kuceyeski, Respino, Hoptman, Scult, Liston, O'Dell, and Gunning report no financial disclosures.

References

Arslan, S., Ktena, S.I., Makropoulos, A., Robinson, E.C., Rueckert, D., Parisot, S., 2018. Human brain mapping: A systematic comparison of parcellation methods for the human cerebral cortex. Neuroimage 170, 5–30. https://doi.org/10.1016/j.neuroimage.2017.04.014

Brandt, J., Benedict, R.H.B., 2001. Hopkins Verbal Learning Test-Revised: Professional Manual. Psychological Assessment Resources.

Braver, T.S., Barch, D.M., Gray, J.R., Molfese, D.L., Snyder, A., 2001. Anterior cingulate cortex and response conflict: Effects of frequency, inhibition and errors. Cereb. Cortex 11, 825–836.

Cahn-Weiner, D.A., Boyle, P.A., Malloy, P.F., 2002. Tests of executive function predict instrumental activities of daily living in community-dwelling older individuals. Appl. Neuropsychol. 9, 187–191. https://doi.org/10.1207/S15324826AN0903_8

Chen, A.C., Oathes, D.J., Chang, C., Bradley, T., Zhou, Z., Williams, L.M., Glover, G.H., Deisseroth, K., Etkin, A., 2013. Causal interactions between fronto-parietal central executive and default-mode networks in humans. Proc. Natl. Acad. Sci. 110, 19944–19949. https://doi.org/10.1073/pnas.1311772110

Cox, R., 1996. AFNI: Software for analysis and visualization of functional magnetic resonance neuroimages. Comput. Biomed. Res. 29, 162–173.

de Chastelaine, M., Wang, T.H., Minton, B., Muftuler, L.T., Rugg, M.D., 2011. The Effects of Age, Memory Performance, and Callosal Integrity on the Neural Correlates of Successful Associative Encoding. Cereb. Cortex 21, 2166–2176. https://doi.org/10.1093/cercor/bhq294

de la Fuente-Fernández, R., 2012. Frontostriatal cognitive staging in Parkinson's disease. Parkinsons. Dis. 2012, 561046. https://doi.org/10.1155/2012/561046

Debette, S., Markus, H.S., 2010. The clinical importance of white matter hyperintensities on brain magnetic resonance imaging: systematic review and meta-analysis. BMJ 341, c3666. https://doi.org/10.1136/bmj.c3666

Drysdale, A.T., Grosenick, L., Downar, J., Dunlop, K., Mansouri, F., Meng, Y., Fetcho, R.N., Zebley, B., Oathes, D.J., Etkin, A., Schatzberg, A.F., Sudheimer, K., Keller, J., Mayberg, H.S., Gunning, F.M., Alexopoulos, G.S., Fox, M.D., Pascual-Leone, A., Voss, H.U., Casey, B.J., Dubin, M.J., Liston, C., 2017. Resting-state connectivity biomarkers define neurophysiological subtypes of depression. Nat. Med. 23, 28–38.

https://doi.org/10.1038/nm.4246

Esposito, R., Cieri, F., Chiacchiaretta, P., Cera, N., Lauriola, M., Di Giannantonio, M., Tartaro, A., Ferretti, A., 2018. Modifications in resting state functional anticorrelation between default mode network and dorsal attention network: comparison among young adults, healthy elders and mild cognitive impairment patients. Brain Imaging Behav. 12, 127–141.

Folstein, M.F., Robins, L.N., Helzer, J.E., 1983. The mini-mental state examination. Arch. Gen. Psychiatry 40, 812–812.

Friedman, N.P., Miyake, A., 2017. Unity and diversity of executive functions: Individual differences as a window on cognitive structure. Cortex 86, 186–204. https://doi.org/10.1016/j.cortex.2016.04.023

Gasquoine, P.G., 2013. Localization of function in anterior cingulate cortex: From psychosurgery to functional neuroimaging. Neurosci. Biobehav. Rev. 37, 340–348. https://doi.org/10.1016/j.neubiorev.2013.01.002

Golden, C.J., Freshwater, S.M., 2002. The Stroop Color and Word Test: A Manual for Clinical and Experimental USes. Stoelting Co., Wood Dale, IL.

Griffanti, L., Zamboni, G., Khan, A., Li, L., Bonifacio, G., Sundaresan, V., Schulz, U.G., Kuker, W., Battaglini, M., Rothwell, P.M., Jenkinson, M., 2016. BIANCA (Brain Intensity AbNormality Classification Algorithm): A new tool for automated segmentation of white matter hyperintensities. Neuroimage 141, 191–205. https://doi.org/10.1016/j.neuroimage.2016.07.018

Gunning-Dixon, F.M., Raz, N., 2003. Neuroanatomical correlates of selected executive functions in middle-aged and older adults: a prospective MRI study. Neuropsychologia 41, 1929–1941. https://doi.org/10.1016/S0028-3932(03)00129-5

Hallquist, M.N., Hillary, F.G., 2018. Graph theory approaches to functional network organization in brain disorders: A critique for a brave new small-world. Netw. Neurosci. 3, 1–26. https://doi.org/10.1162/netn

Jenkinson, M., Beckmann, C.F., Behrens, T.E.J., Woolrich, M.W., Smith, S.M., 2012. FSL. Neuroimage 62, 782–790. https://doi.org/10.1016/j.neuroimage.2011.09.015

Klostermann, E.C., Braskie, M.N., Landau, S.M., O'Neil, J.P., Jagust, W.J., 2012. Dopamine and frontostriatal networks in cognitive aging. Neurobiol. Aging 623.e15-623.e24. https://doi.org/10.1016/j.neurobiolaging.2011.03.002

Koshino, H., Minamoto, T., Yaoi, K., Osaka, M., Osaka, N., 2014. Coactivation of the Default Mode Network regions and Working Memory Network regions during task preparation. Sci. Rep. 4, 5954. https://doi.org/10.1038/srep05954

Kuceyeski, A., Maruta, J., Relkin, N., Raj, A., 2013. The Network Modification (NeMo) Tool: Elucidating the Effect of White Matter Integrity Changes on Cortical and Subcortical Structural Connectivity. Brain Connect. 3, 451–463. https://doi.org/10.1089/brain.2013.0147

Kuceyeski, A., Navi, B.B., Kamel, H., Relkin, N., Villanueva, M., Raj, A., Toglia, J., O'Dell, M.W., Iadecola, C., 2015. Exploring the brain's structural connectome: A quantitative stroke lesion-dysfunction mapping study. Hum. Brain Mapp. 36, 2147–2160. https://doi.org/10.1002/hbm.22761

Kuceyeski, A., Zhang, Y., Raj, A., 2012. Linking white matter integrity loss to associated cortical regions using structural connectivity information in Alzheimer's disease and fronto-temporal dementia: The Loss in Connectivity (LoCo) score. Neuroimage 61, 1311–1323. https://doi.org/10.1016/j.neuroimage.2012.03.039

Langen, C.D., Cremers, L.G.M., de Groot, M., White, T., Ikram, M.A., Niessen, W.J., Vernooij, M.W., 2018. Disconnection due to white matter hyperintensities is associated with lower cognitive scores. Neuroimage 183, 745–756. https://doi.org/10.1016/j.neuroimage.2018.08.037

Leech, R., Sharp, D.J., 2014. The role of the posterior cingulate cortex in cognition and disease. Brain 137, 12–32. https://doi.org/10.1093/brain/awt162

Liem, F., Varoquaux, G., Kynast, J., Beyer, F., Kharabian Masouleh, S., Huntenburg, J.M., Lampe, L., Rahim, M., Abraham, A., Craddock, R.C., Riedel-Heller, S., Luck, T., Loeffler, M., Schroeter, M.L., Veronica, A.V., Villringer, A., Margulies, D.S., 2017. Predicting brain-age from multimodal imaging data captures cognitive impairment. Neuroimage 148, 179–188. https://doi.org/10.1016/j.neuroimage.2016.11.005

Mehmood, T., Liland, K.H., Snipen, L., Sæbø, S., 2012. A review of variable selection methods in Partial Least Squares Regression. Chemom. Intell. Lab. Syst. 118, 62–69.

Moroni, F., Ammirati, E., Rocca, M.A., Filippi, M., Magnoni, M., Camici, P.G., 2018. Cardiovascular disease and brain health: Focus on white matter hyperintensities. IJC Hear. Vasc. 19, 63–69. https://doi.org/10.1016/j.ijcha.2018.04.006

Pantsiou, K., Sfakianaki, O., Papaliagkas, V., Savvoulidou, D., Costa, V., Papantonoiu, G., Moraitou, D., 2018. Inhibitory Control, Task/Rule Switching, and Cognitive Planning in Vascular Dementia: Are There Any Differences From Vascular Aging ? Front. Aging Neurosci. 10, 1–17. https://doi.org/10.3389/fnagi.2018.00330

Power, J.D., Cohen, A.L., Nelson, S.M., Wig, G.S., Barnes, K.A., Church, J.A., Vogel, A.C., Laumann, T.O., Miezin, F.M., Schlaggar, B.L., Petersen, S.E., 2011. Functional network organization of the human brain. Neuron 72, 665–678. https://doi.org/10.1016/j.neuron.2011.09.006

Pruim, R.H.R., Mennes, M., van Rooij, D., Llera, A., Buitelaar, J.K., Beckmann, C.F., 2015. ICA-AROMA: A robust ICA-based strategy for removing motion artifacts from fMRI data. Neuroimage 112, 267–277. https://doi.org/10.1016/j.neuroimage.2015.02.064

Reijmer, Y.D., Schultz, A.P., Leemans, A., O'Sullivan, M.J., Gurol, M.E., Sperling, R., Greenberg, S.M., Viswanathan, A., Hedden, T., 2015. Decoupling of structural and functional brain connectivity in older adults with white matter hyperintensities. Neuroimage 117, 222–229. https://doi.org/10.1016/j.neuroimage.2015.05.054

Reitan, R.M., 1958. Validity of the Trail Making Test as an Indicator or Organic Brain Damage. Percept. Mot. Skills 8, 271–276. https://doi.org/10.2466

Respino, M., Jaywant, A., Kuceyeski, A., Victoria, L.W., Hoptman, M.J., Scult, M.A., Sankin, L., Pimontel, M., Liston, C., Belvederi Murri, M., Alexopoulos, G.S., Gunning, F.M., 2019. The impact of white matter hyperintensities on the structural connectome in late-life depression: Relationship to executive functions. NeuroImage Clin. https://doi.org/10.1016/j.nicl.2019.101852

Salthouse, T.A., 2011. What cognitive abilities are involved in trail-making performance? Intelligence 39, 222–232. https://doi.org/10.1016/j.intell.2011.03.001.What

Schaefer, A., Quinque, E.M., Kipping, J.A., Arelin, K., Roggenhofer, E., Frisch, S., Villringer, A., Mueller, K., Schroeter, M.L., 2014. Early small vessel disease affects frontoparietal and cerebellar hubs in close correlation with clinical symptoms — a resting-state fMRI study. J. Cereb. Blood Flow Metab. 34, 1091–1095. https://doi.org/10.1038/jcbfm.2014.70

Skudlarski, P., Jagannathan, K., Anderson, K., Stevens, M.C., Calhoun, V.D., Skudlarska, B.A., Pearlson, G., 2010. Brain Connectivity Is Not Only Lower but Different in Schizophrenia: A Combined Anatomical and Functional Approach. Biol. Psychiatry 68, 61–69.

https://doi.org/10.1016/j.biopsych.2010.03.035

Sun, Y., Qin, L., Zhou, Y., Xu, Q., Qian, L., Tao, J., Xu, J., 2011. Abnormal functional connectivity in patients with vascular cognitive impairment, no dementia: A resting-state functional magnetic resonance imaging study. Behav. Brain Res. 223, 388–394. https://doi.org/10.1016/j.bbr.2011.05.006

Tombaugh, T.N., 2006. A comprehensive review of the Paced Auditory Serial Addition Test (PASAT). Arch. Clin. Neuropsychol. 21, 53–76. https://doi.org/10.1016/j.acn.2005.07.006

Tuladhar, A.M., van Dijk, E., Zwiers, M.P., van Norden, A.G.W., de Laat, K.F., Shumskaya, E., Norris, D.G., de Leeuw, F.-E., 2016. Structural Network Connectivity and Cognition in Cerebral Small Vessel Disease. Hum. Brain Mapp. 37, 300–310. https://doi.org/10.1002/hbm.23032

Vatansever, D., Manktelow, A.E., Sahakian, B.J., Menon, D.K., Stamatakis, E.A., 2017. Angular Default Mode Network connectivity across working memory load. Hum. Brain Mapp. 38, 41–52. https://doi.org/10.1002/hbm.23341

Vaughan, L., Giovanello, K., 2010. Executive function in daily life: Age-related influences of executive processes on instrumental activities of daily living. Psychol. Aging 25, 343–355. https://doi.org/10.1037/a0017729

Wahlund, L.O., Barkhof, F., Fazekas, F., Bronge, L., Augustin, M., Sjögren, M., Wallin, A., Ader, H., Leys, D., Pantoni, L., Pasquier, F., Erkinjuntti, T., Scheltens, P., 2001. A new rating scale for age-related white matter changes applicable to MRI and CT. Stroke 32, 1318–1322. https://doi.org/10.1161/01.STR.32.6.1318

Wechsler, D., 2008. Wechsler Adult Intelligence Scale-Fourth Edition (WAIS-IV). Pearson, San Antonio, TX.

Wiseman, S.J., Booth, T., Ritchie, S.J., Cox, S.R., Munoz Maniega, S., del C Valdes Hernandez, M., Dickie, D.A., Royle, N.A., Starr, J.M., Deary, I.J., Wardlaw, J.M., Bastin, M.E., 2018. Cognitive Abilities, Brain White Matter Hyperintensity Volume , and Structural Network Connectivity in Older Age. Hum. Brain Mapp. 39, 622–632. https://doi.org/10.1002/hbm.23857

Xiong, Y., Yang, J., Wong, A., Wong, C.H.K., Chan, S.S.W., Li, H.H.S., Tam, L.H.P., Bao, J.W.K., Wong, G.C.Y., Chen, X., Chu, W.C.W., Lee, W.K., Wong, K.S., Mok, V.C.T., 2011. Operational definitions improve reliability of the age-related white matter changes

scale. Eur. J. Neurol. 18, 744–749. https://doi.org/10.1111/j.1468-1331.2010.03272.x

Xu, X., Tang, R., Zhang, L., Cao, Z., 2019. Altered Topology of the Structural Brain Network in Patients With Post-stroke Depression. Front. Neurosci. 13, 776. https://doi.org/10.3389/fnins.2019.00776

Yi, L., Liang, X., Liu, D., Sun, B., Ying, S., Yang, D., Li, Q., Jiang, C., Han, Y., 2015. Disrupted Topological Organization of Resting-State Functional Brain Network in Subcortical Vascular Mild Cognitive Impairment. CNS Neurosci. Ther. 21, 846–854. https://doi.org/10.1111/cns.12424

Zimmermann, J., Ritter, P., Shen, K., Rothmeier, S., Schirner, M., Mcintosh, A.R., 2016. Structural Architecture Supports Functional Organization in the Human Aging Brain at a Regionwise and Network Level. Hum. Brain Mapp. 2661, 2645–2661. https://doi.org/10.1002/hbm.23200

Zuo, X., Xing, X., 2014. Test-retest reliabilities of resting-state FMRI measurements in human brain functional connectomics: A systems neuroscience perspective. Neurosci. Biobehav. Rev. 45, 100–118.

Table 1. Demographic and clinical characteristics of the study sample.

	Mean	SD	Minimum	Maximum
Age	72.9	6.02	60	84
Education	16.9	2.23	12	20
Gender (M/F)	33/25	--	--	--
Stroop Interference	-3.80	7.73	-27.6	12.9
TMT B/A Ratio	2.42	0.93	0.40	5.41
Digit Span Total	15.3	3.55	9	25
HVLT-R Delayed Recall	8.84	2.17	0	12

Table 2. Region pairs in which WMH-associated dysconnectivity score (0 to -1, more negative = greater inferred loss of connectivity) was significantly correlated with performance on the Stroop task after FDR-correction (q < .05). Positive correlations indicate that less dysconnectivity is associated with better performance. Also shown are functional nodes from the modified Power parcellation that overlapped with these region pairs and significantly correlated with Stroop performance. Note that some Power nodes are represented in multiple region pairs because they overlap with the boundaries from the atlas used to calculate dysconnectivity scores.

Region Pair	Correlation between dysconnectivity score and Stroop performance (Spearman rho)	Significance (FDR-corrected p)	MNI coordinates [x, y, z] of functional nodes within the region pair that are significantly associated with Stroop performance (Spearman rho, uncorrected p)	Correlation between dysconnectivity score and RSFC within the region pair (Spearman rho, uncorrected p)
Right Caudate – Right Inferior Parietal	.38	.036	[11, 6, -6]–[44, -53, 47], rho= .27, p=.04 [11, 6, -6]–[37, -65, 40], rho= .33, p=.01	rho=.22, p=.10 rho=.18, p=.17
Right Caudate – Right Superior Parietal	.38	.036	[15, 5, 7]–[22, -42, 69], rho= .27, p=.04	rho=.16, p=.25
Right Caudate – Right Supramarginal Gyrus	.42	.022	[11, 6, -6]–[47, -30, 49], rho= -.38, p=.003	rho= -.24, p=.07
Right Caudate – Right Posterior Cingulate	.42	.022	[11, 6, -6]–[47, -30, 49], rho= -.38, p=.003	rho= -.14, p=.31
Left Pars Triangularis – Left Medial Orbitofrontal	.38	.039	[-42, 45, -2]–[-3, 44, -9], rho= -.30, p=.02	rho=.07, p=.59
Right Thalamus – Right Superior Frontal Gyrus	.43	.022	None	--
Right Pallidum – Right Superior Frontal Gyrus	.41	.023	[15, 5, 7]–[6, 54, 16], rho= -.27, p=.04	rho= -.13, p=.35

Left Lateral Orbitofrontal – Left Anterior Cingulate Cortex	.40	.026	None	--
Right Caudate – Right Insula	.41	.023	None	--
Right thalamus – Right caudal middle frontal	.43	.022	None	--
Right Caudate – Right Caudal Middle Frontal	.42	.022	[15, 5, 7]–[47, 10, 33], rho= .29, p=.03	rho=.25, p=.06
Right Caudate – Right Paracentral	.43	.022	None	--
Right Caudate – Right Postcentral Gyrus	.43	.022	[11, 6, -6]–[47, -30, 49], rho= -.38, p=.003	rho= -.21, p=.11
Right Thalamus – Right Precentral Gyrus	.37	.047	None	--
Right Caudate – Right Precentral Gyrus	.48	.022	[15, 5, 7]–[47, 10, 33], rho= .29, p=.03 [12, 18, -3]–[47, 10, 33], rho= .26, p=.04	rho=.19, p=.15 rho=.29, p=.03
Right Caudate – Right Putamen	.41	.023	None	--

Figure 1.

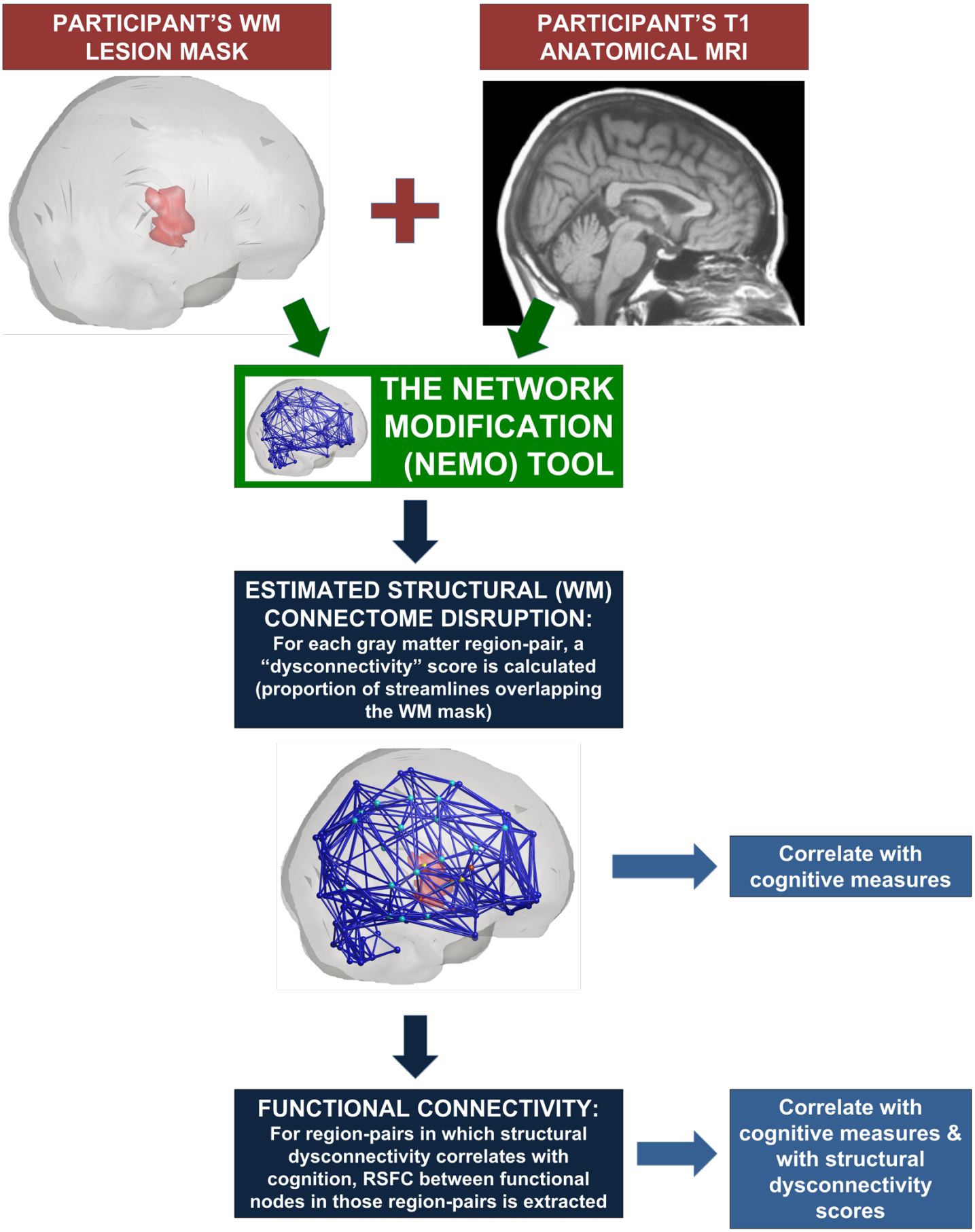
PARTICIPANT'S WM LESION MASK
PARTICIPANT'S T1 ANATOMICAL MRI
THE NETWORK MODIFICATION (NEMO) TOOL
ESTIMATED STRUCTURAL (WM) CONNECTOME DISRUPTION:
For each gray matter region-pair, a "dysconnectivity" score is calculated (proportion of streamlines overlapping the WM mask)
Correlate with cognitive measures
FUNCTIONAL CONNECTIVITY:
For region-pairs in which structural dysconnectivity correlates with cognition, RSFC between functional nodes in those region-pairs is extracted
Correlate with cognitive measures & with structural dysconnectivity scores

Figure 2.

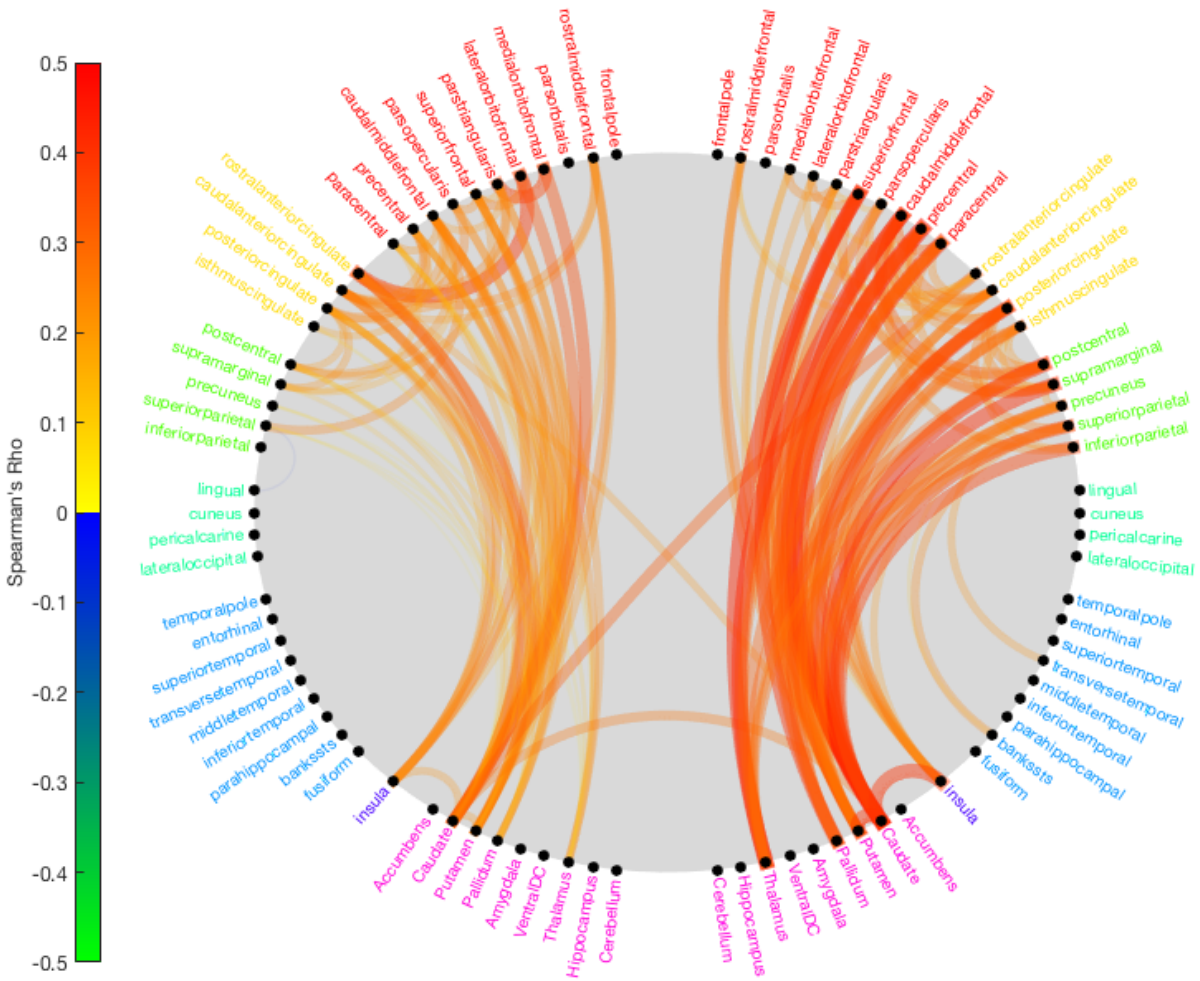
Spearman's Rho
0.5
0.4
0.3
0.2
0.1
0
-0.1
-0.2
-0.3
-0.4
-0.5
frontalpole
rostralmiddlefrontal
parsorbitalis
medialorbitofrontal
lateralorbitofrontal
parstriangularis
superiorfrontal
parsopercularis
caudalmiddlefrontal
precentral
paracentral
rostralanteriorcingulate
caudalanteriorcingulate
posteriorcingulate
isthmuscingulate
postcentral
supramarginal
precuneus
superiorparietal
inferiorparietal
lingual
cuneus
pericalcarine
lateraloccipital
temporalpole
entorhinal
superiortemporal
transversetemporal
middletemporal
inferiortemporal
parahippocampal
bankssts
fusiform
insula
Accumbens
Caudate
Putamen
Pallidum
Amygdala
VentralDC
Thalamus
Hippocampus
Cerebellum

Figure 3

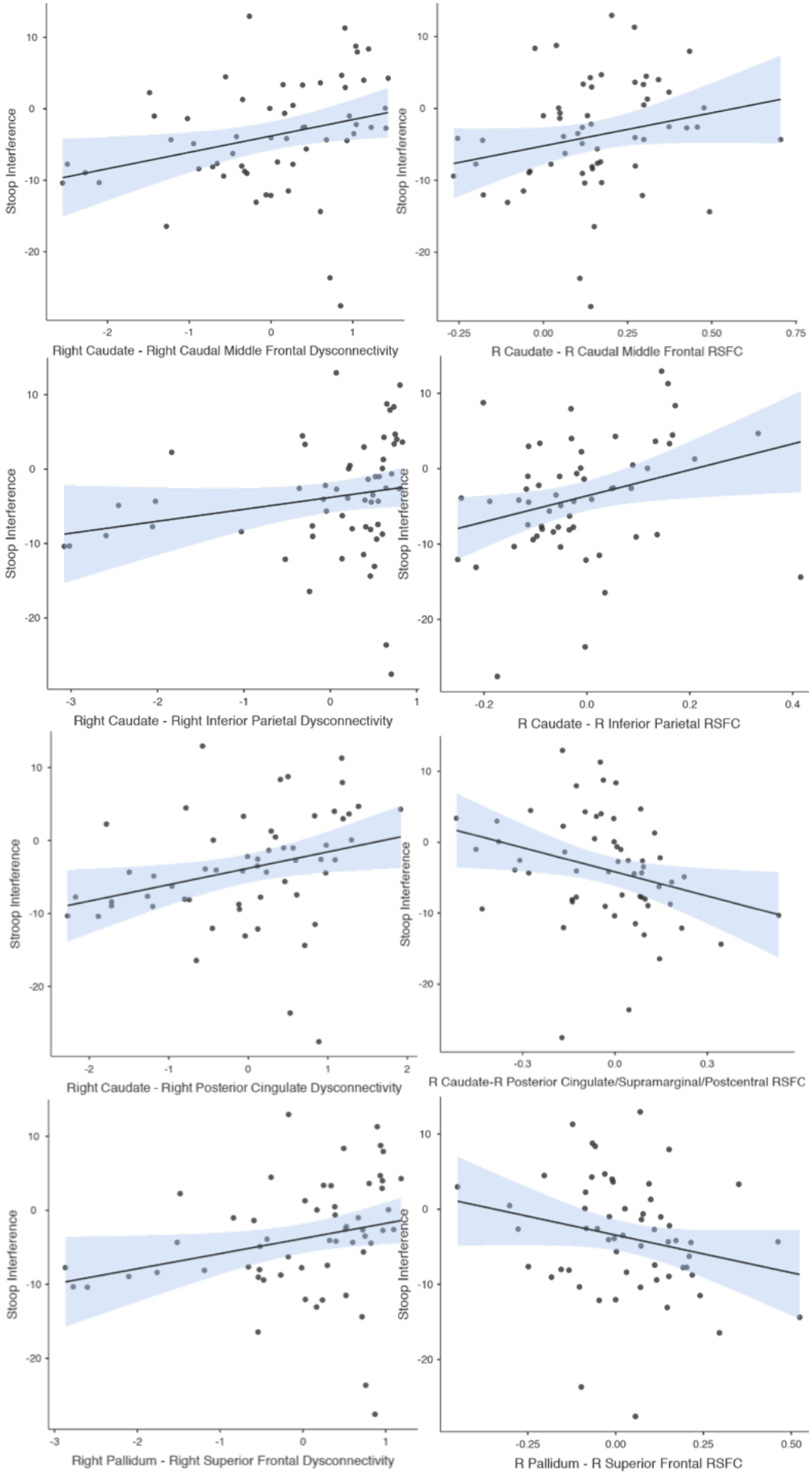
Stoop Interference
Right Caudate - Right Caudal Middle Frontal Dysconnectivity
R Caudate - R Caudal Middle Frontal RSFC
Right Caudate - Right Inferior Parietal Dysconnectivity
R Caudate - R Inferior Parietal RSFC
Stroop Interference
Right Caudate - Right Posterior Cingulate Dysconnectivity
R Caudate-R Posterior Cingulate/Supramarginal/Postcentral RSFC
Right Pallidum - Right Superior Frontal Dysconnectivity
R Pallidum - R Superior Frontal RSFC

Figure 4

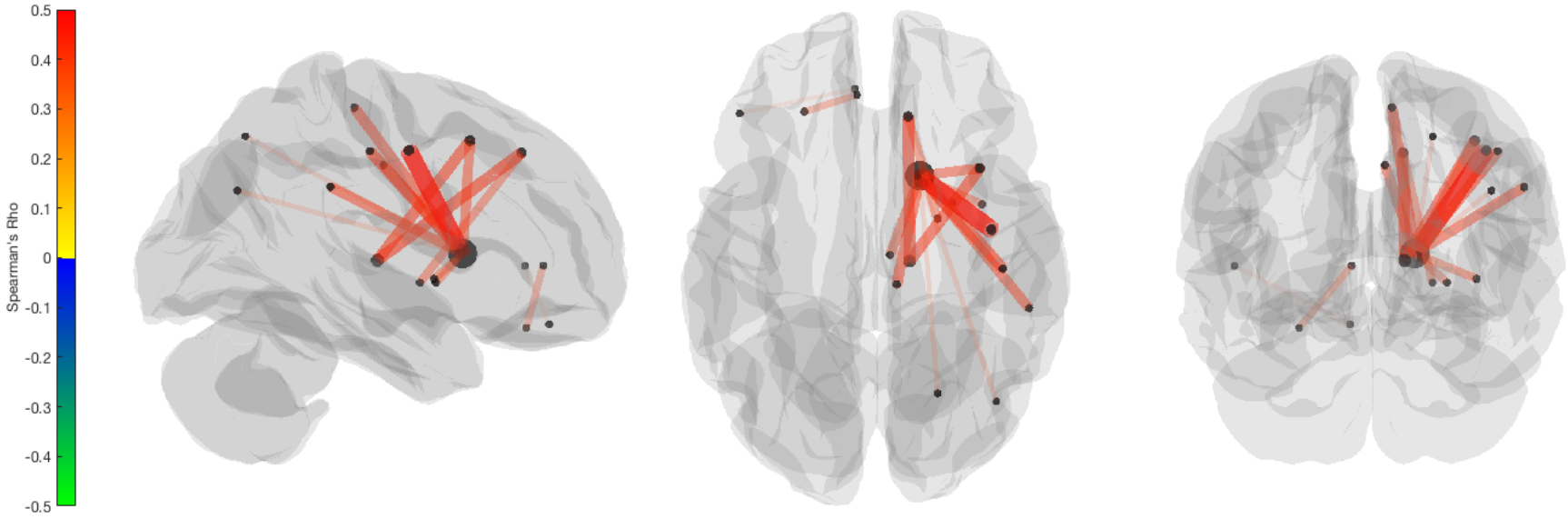

Figure 5

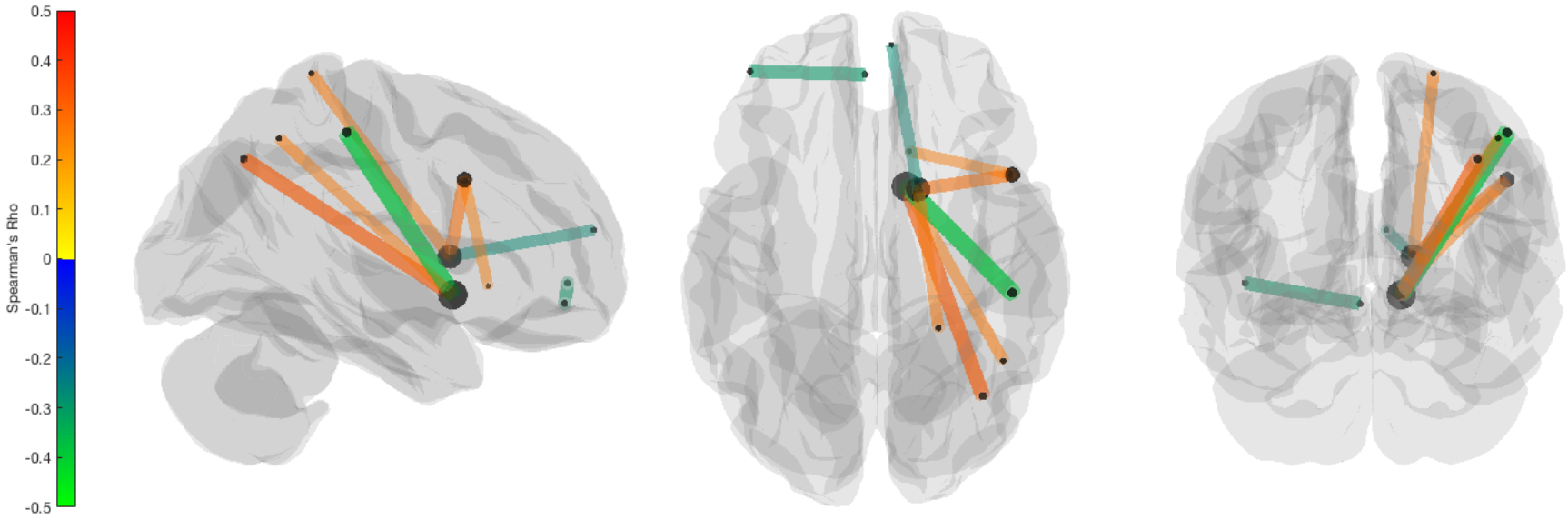

Figure Captions

Figure 1. Flowchart of neuroimaging analysis procedures and statistical procedures for the primary analyses.

Figure 2. Scatterplots (with best fit lines and standard errors) depicting the relationship between Stroop performance, inferred structural dysconnectivity, and resting state functional connectivity.

Figure 3. Schematic representing the correlation between inferred structural dysconnectivity in all 170 region-pairs and performance on the Stroop task. ROIs are grouped by region and by hemisphere. Warm colors represent positive correlation coefficients that indicate a relationship in the expected direction, whereby lower dysconnectivity scores (i.e., more negative values and more inferred loss in connectivity) are associated with poorer Stroop performance and vice-versa.

Figure 4. Glassbrains representing the correlation between Stroop performance and inferred structural dysconnectivity in those region-pairs that survived FDR-correction. Warm colors represent positive correlation coefficients that indicate a relationship in the expected direction, whereby lower dysconnectivity scores (i.e., more negative values and more inferred loss in connectivity) are associated with poorer Stroop performance and vice-versa.

Figure 5. Glassbrains representing the correlation between Stroop performance and resting state functional connectivity (RSFC) in functional nodes that overlap with ROIs that emerged as significant in structural analyses. Warm colors represent positive correlation coefficients that indicate that greater RSFC is associated with better Stroop performance. Cool colors represent negative correlation coefficients.